Am J Cancer Res 2024;14(7):3419-3432
www.ajcr.us /ISSN:2156-6976/ajcr0157772

Original Article

LGR4 attenuates MGP expression and suppresses EGFR activation-induced triple-negative breast cancer metastasis

Qishuang Li[1*], Yankun Gao[2*], Zitian Huo[3], Jing Liu[2], Pumin Zhang[1], Yi Wang[2]

[1]State Key Laboratory of Targeting Oncology, National Center for International Research of Biotargeting Theranostics, Guangxi Key Laboratory of Biotargeting Theranostics, Collaborative Innovation Center for Targeting Tumor Diagnosis and Therapy, Guangxi Medical University, Nanning 530021, Guangxi, PR China; [2]State Key Laboratory of Proteomics, Beijing Proteome Research Center, National Center for Protein Sciences (Beijing), Beijing Institute of Lifeomics, Beijing 102206, PR China; [3]Institute of Pathology, Tongji Hospital, Huazhong University of Science and Technology, Wuhan 430030, Hubei, PR China. [*]Equal contributors.

Received May 14, 2024; Accepted July 2, 2024; Epub July 15, 2024; Published July 30, 2024

Abstract: Breast cancer has emerged as the most common cancer globally, with a significant reduction in overall survival rate after metastasis. Compared with other types of breast cancer, triple-negative breast cancer (TNBC) is more prone to metastasize, presenting substantial treatment challenges due to the lack of effective therapies. LGR4, which is highly expressed in breast cancer, has been shown to promote the proliferation and invasion of breast cancer cells. However, its specific role in TNBC remains unclear. In this study, we applied a multi-omics approach to explore the regulatory mechanism of LGR4 in TNBC metastasis. Our findings showed that LGR4 could regulate actin cytoskeletal through EGFR and curtail EGFR activation-induced TNBC metastasis by inhibiting MGP expression. These insights provide new perspectives on the role of LGR4 in breast cancer metastasis.

Keywords: Breast cancer, EGFR, LGR4, MGP

Introduction

According to the latest global cancer statistics from International Agency for Research on Cancer (IARC) of the World Health Organization's in 2021, breast cancer remains one of the most prevalent cancers worldwide, with a high mortality rate among female cancers. Up to 30% of breast cancer patients exhibit metastases prior to diagnosis, dramatically affecting survival rates. While the 5-year survival rate for non-metastatic breast cancer is higher than 80% [1, 2], this rate decreases to about 25% after distant metastases [3]. Breast cancer tends to metastasize to different organs, including bone, lung, liver, brain, among which the number of cases of bone metastasis is 75% [4] and the 5-year overall survival rate is about 22.8% [5].

Triple-negative breast cancer (TNBC), known for its high metastatic potential [6], lacks effective treatment options, making management particularly challenging in metastatic cases [7, 8]. Therefore, exploring the mechanism of breast cancer metastasis and identifying related molecules will provide targets for developing targeted therapies and improve clinical outcomes.

LGR4 plays a key role in various physiological processes such as cell development and stemness maintenance. Its aberrant expression has been associated with the occurrence and progression of a variety of diseases [9]. LGR4 deletion in neonatal mice leads to defects in the development of multiple organs, such as reproductive function [10], kidney, hair follicle, gallbladder, intestine, and skin [11, 12]. It also binds to RANKL to inhibit mouse osteoclast differentiation and activity [13]. LGR4 is highly expressed in breast cancer [14] and has been associated with promoting the proliferation and invasion of breast cancer cells [15]. However, its role in TNBC remains under-studied.

https://doi.org/10.62347/THII9650

RANKL and R-spondin 2 (RSPO2) are known to interact with the receptor LGR4 to regulate the WNT inhibitor DKK1 through Gαq and β-catenin signaling. This interaction promotes the formation of premetastatic niches in osteoclasts and enhances bone metastasis in breast cancer [16]. Although existing studies have shown that LGR4 functions primarily through the wnt pathway [17], it also has been demonstrated that LGR4 can promote breast cancer metastasis independently of this pathway. By interacting with EGFR, LGR4 enhances EGFR signaling transduction, further promoting breast cancer metastasis [18].

The ERBB family of receptor tyrosine kinases (RTKs) consists of four members: EGFR (epidermal growth factor receptor, also known as ERBB1/HER1), ERBB2 (HER2), ERBB3 (HER3), and ERBB4 (HER4). These cytoplasmic membrane-anchored proteins share structural and sequence similarities, each containing an extracellular ligand-binding domain, a transmembrane domain, and intracellular tyrosine kinase domain. In cancer, EGFR often undergoes uncontrolled auto-phosphorylation, resulting in increased cellular proliferation and reduced apoptosis. Overexpression of EGFR is observed in 15-30% of breast carcinoma, correlating with large tumor size and poor clinical outcomes. Notably, EGFR expression is particularly higher in TNBC [19]. The aberrant activation of EGFR in cancer typically results from point mutations and overexpression, though transcriptional upregulation or ligand overproduction via juxtacrine, autocrine, paracrine and/or endocrine signaling mechanisms has also been observed [20]. In this study, EGF was used to stimulate TNBC cells in order to mimic non-genomical activation of EGFR in tumor microenvironment.

MGP, a member of the stromal cell protein family, plays an important role in bone homeostasis and coagulation [21]. It has been shown to affect the cross-linking of the extracellular matrix as well as the migration, adhesion, and proliferation of various cells including osteoblasts, epithelial cells, fibroblasts, and cardiomyocytes [22, 23]. Research by Gong Chen et al. showed that HOXC8 interacts with MGP to promote proliferation, migration, and EMT of TNBC cells [24]. However, the role of MGP in breast cancer progression, particularly in relation to LGR4 and its regulatory effects on cell migration, remains poorly understood.

In this study, we investigated how LGR4 impacts EGFR-associated complex in TNBC cell line and further examined the role of MGP in cell migration. Our results suggest a potential regulatory mechanism involving LGR4-EGFR signaling that could influence metastasis in TNBC cells.

Materials and methods

Antibodies and reagents

Dulbecco's modified Eagle medium (DMEM), RPMI-1640 medium and fetal bovine serum (FBS) were sourced from Gibco (Grand Island, New York). The following antibodies were used in Western Blotting (WB): LGR4 (Cat No. sc-390639, 1:1000, Santa Cruz Biotechnology), GAPDH (Cat No. 60004-1-1g, 1:5000, proteintech, Wuhan, China), MGP (Cat No. 10734-1-AP, 1:100, proteintech, Wuhan, China), and additional LGR4 (Cat No. 20150-1-AP, 1:100, proteintech, Wuhan, China). EGF and formaldehyde were purchased from Sigma-Aldrich and Protein A-Sepharose beads (17-0780-01, GE Healthcare, Piscataway, NJ) were used for immunoprecipitation.

Cell culture and treatment

MDA-MB-468 and LGR4-KO breast cancer cells were provided by Y Li. HEK 293T cells and MDA-MB-468 cells were cultured in DMEM (Sigma) supplemented with 10% FBS and 1% Pen-Strep (100 units/ml penicillin and 100 mg/ml streptomycin). Both WT and LGR4 KO MDA-MB-468 cells, when 80% confluent, were serum-starved for 24 h before stimulation with 50 ng/mL EGF for designated times.

Quantitative real-time PCR (QPCR) analysis

Cells were collected in Trizol, and chloroform was used for phase separation. An equal volume of pre-cooled isopropanol was added for RNA precipitation, followed by centrifugation. The RNA pellet was washed twice with pre-cooled 75% absolute ethanol, air-dried in a biosafety cabinet, and dissolved in RNase-free water. The concentration of RNA was determined, and the RNA was then used for reverse transcription with 5X RT Master Mix. QPCR was performed using SYBR Premix Ex Taq II, specific

primers (listed in Table S1), and the extracted cDNA. The amplification curve and melting curve were analyzed to confirm the specificity and efficiency of amplification.

Western blot (WB) analysis

Post-treatment, cells were lysed with the lysis buffer (50 mM Tris-HCl, 150 mM NaCl, 1% Triton X-100, and 0.1% SDS) supplemented with protease inhibitors (Roche). The protein concentration was quantified using the BCA assay. Protein was separated by SDS-PAGE gel, transferred to the nitrocellulose membrane, and blocked with 5% non-fat milk in TBST for 1 h at room temperature. Primary antibodies were applied overnight at 4°C, followed by secondary antibody for 1 hr at room temperature. Protein bands were visualized using chemiluminescent substrates and either X-ray films or a CCD camera (Tanon 5200 Luminescent Imaging Workstation).

Cross-linking and membrane protein extract

Formaldehyde was added directly to the culture medium to achieve a final concentration of 1% and was cross-linked for 8 minutes at 37°C in the incubator. Cross-linking was quenched by adding glycine to a final concentration of 200 mM for 4 minutes at room temperature. The membrane proteins were extracted by re-suspending the pellet in RIPA buffer (10 mM Tris-HCl [pH 8.0], 140 mM NaCl, 1 mM EDTA, 0.5 mM EGTA, 1% Triton X-100, 0.1% SDS, 0.1% Sodium deoxycholate, phosphatase inhibitor, and protease inhibitor cocktails) for 30 minutes on ice followed by sonication using a Sonics Ultrasonic Processors VCX. After centrifugation for 15 minutes at 14,000 g, the supernatant concentration was quantified by a BCA assay and used for immunoprecipitation (IP) experiments.

Immunoprecipitation

For each IP experiment, at least 1 mg of protein lysate was incubated with 5 ug of antibody for 2 hours at 4°C with rotation, followed by ultracentrifugation at 60,000 g for 15 minutes to clear the mixture. The supernatant was then incubated with Protein A beads for 1 hour at 4°C with rotation. The beads were washed four times with NETN buffer (20 mM Tris [pH 7.5], 1 mM EDTA, 0.5% NP-40, and 150 mM NaCl) to reduce non-specific protein binding. Samples were then mixed with 2 × SDS loading buffer and incubated at 60°C for 30 minutes. IP Samples were resolved on a 10% SDS-PAGE Acr-Bis 10-well gel and stained with Coomassie Brilliant Blue for 10 minutes, then decolorized either by shaking for 2 hours or overnight in water. Gels were cut into 3 molecular weight regions including an IgG heavy and a light chain band. The gel pieces were destained by changing the solution until transparent, then dehydrated with 70% acetonitrile 200 µl for 30 minutes, followed by rehydration in 300 µl 50 mM NH_4HCO_4 for 5 minutes. Each band was digested in gel with 200 ng of trypsin in 20 µL of 50 mM NH_4HCO_3 overnight at 37°C. Peptides were extracted with 200 µl of 100% acetonitrile, intermittently rehydrated in 30 µl of 0.1% formic acid (FA), and then dried in a Speed-Vac. Digested peptides were dissolved in 10 µl of loading solution (5% methanol containing 0.1% FA).

Mass spectrometry and protein quantification

Peptide samples were analyzed using an Orbitrap Fusion mass spectrometer connected to an EASY-nLC 1200 system. The system includes pre-columns (20 mm long × 100 µm I.D, with C18 packing material 3 µm diameter), separation columns (column I.D: 150 mm long × 150 µm, with C18 packing material 1.9 µm diameter), quadrupoles, and ion traps. The mobile phase can be divided into two phases: Phase A, which consists of 0.1% FA in water, and Phase B, which consists of 0.1% FA in an acetonitrile aqueous solution (20% acetonitrile + 80% mass spectrometry water). The sample elution occurs at a flow rate of 600 nL/min over a 5-35% nonlinear gradient. Peptides are eluted by analytical columns and ionized by an electrospray ion source. They were subjected to a full scan (300-1400 m/z; 200 m/z; R = 60000) under an automated gain-controlled target of 3e6 ions, followed by up to 20 data-dependent MS/MS scans using higher energy collisional dissociation (HCD) in Orbitrap (200 m/z, R = 15000). The primary acquisition mass range for the fragmentation mode is 350-1500 Da.

Transwell migration analysis

For cells maintained in good culture, incubate with serum-depleted medium for 12 hours to

eliminate the serum effects. After trypsinizing the cells, collect 1 × 10^5 cells and resuspend them in 200 μl serum-free medium. Add 600 μl of DMEM medium (containing serum) to the lower chamber of a 24-well plate. Place the transwell inserts into a 24-well plate with 3 replicates per set of experiments. Transfer the cell suspension into the transwell chamber and incubate in a cell culture incubator for 24 hours. Following incubation, remove the non-migrating cells from the transwell membrane with a cotton swab. Fix the cells with 4% paraformaldehyde (PFA) for 30 minutes. Stain the cells with 0.1% crystal violet for 30 minutes, washed three times with PBS, and wipe off the residual PBS with a cotton swab. After being left to dry at room temperature, 6-8 10 × fields of view were randomly selected for each compound well, and the number of cells in each field was counted and plotted.

Profiling sample preparation

Cells were cultured with 3 replicates in parallel. Starve the cells for 18 hours and collect 1 ml of medium supernatant. Centrifuge at 16,000 g, then add 100 μl of supernatant to 10 ug of trypsin and incubate overnight in a 37°C incubator for enzymatic digestion. Add 0.5 μl FA to the mixture, centrifuge, and collect the supernatant. For desalting, transfer the sample to a vacuum dryer at 60°C. After 2 hours, the liquid was drained to obtain dry powdered peptides, which were stored at 4°C for mass spectrometry analysis.

Data analysis

Raw data was processed using the laboratory's own search engine Firmiana, against the NCBI human Ref-sequence protein database (updated in July 2013, containing 34,297 proteins), applying a 1% false discovery rate (FDR) criterion. The peptide ion tolerance was set at 20 ppm for MS1 and 0.5 Da for MS2, allowing a maximum of 2 missed cleavage sites and a minimum peptide length of 7 amino acids. Dynamic modifications in IP-MS included acetylation (Protein N-term), oxidation (M), and DeStreak (C). The quantitative method is intensity-based absolute quantification (iBAQ), which is based on the area under the curve (AUC) ratio of the peptide to the number of theoretical peptides as the iBAQ value of each protein identified. Raw was used for further exploration, statistical analysis, and visualization.

Results

LGR4 knockout inhibited the migration ability of TNBC cell lines

We initially evaluated the efficiency of LGR4 knockout in cell lines (**Figure 1A**, **1B**). Subsequently, we assessed the migration of LGR4 in MDA-MB-468 TNBC cells (control and knockout). Cells were subjected to transwell assay following 12 hours of serum starvation. We observed that the migration of the LGR4 knockout cell line was significantly reduced compared to the control group (**Figure 1C**), with a statistically significant *P* value as shown in the histogram of **Figure 1D**. These findings confirm that LGR4 knockout inhibits the migration of TNBC cell lines, corroborating with previous published data.

Omics analysis showed LGR4 knockout affected EGFR-interacting proteins and kinetics

LGR4 is known to interact with EGFR without independently of the Wnt pathway, promoting breast cancer metastasis by preventing EGFR ubiquitination and degradation [18]. However, the mechanism through which LGR4 regulates the downstream EGFR pathway remains underexplored. We used IP-XL/MS and CRISPR/Cas9 to investigate dynamic changes in EGFR signaling pathway and to explore EGFR and LGR4-associated PPIs in TNBC. Utilizing a crosslinking protocol used by Chen et al., we aimed to obtain reproducible results in capturing the weak and transient interacting proteins within an extended EGFR proteome [25].

We applied the Fast Sequence Proteomics Workflow (**Figure 2**), a label-free quantitative proteomics approach, and identified 4986 gene products (GPs) with a 1% peptide false discovery rate (FDR), as shown in **Figure 3A**. Among these (Table S2), LGR4 was significantly knocked out notably under EGF stimulation (**Figure 3B**). A total of 417 EGF-inducible GPs (Table S3) were identified as high-quality IDs by selecting those that have been measured with at least two unique peptides (GPs-specific sequences) and three stringent peptides (mascot ion score ≥ 20) with a twofold change (**Figure 3C**), illustrated in the heatmap (**Figure 3D**). Subsequently, we compared the results between WT and LGR4 knockout stable strains across different EGF stimulation time points, as shown in the Venn diagram (**Figure 3E**). A total

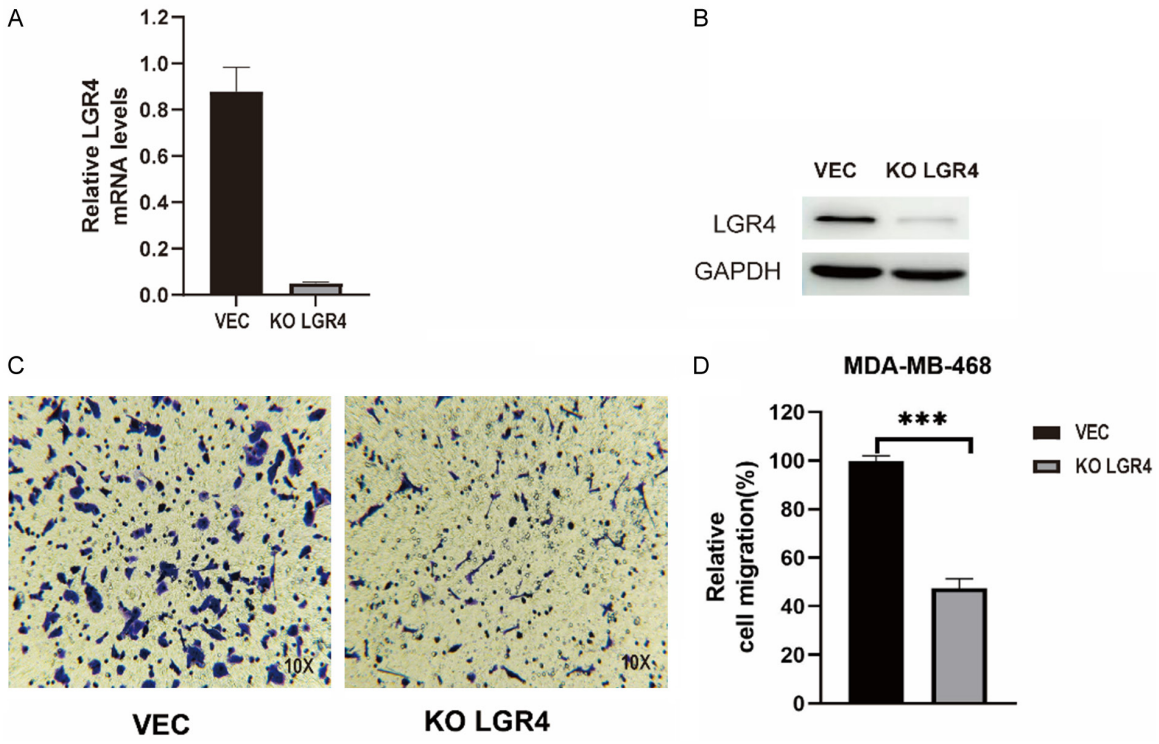

Figure 1. LGR4 knockout reduces breast cancer cell migration. (A) QPCR analysis in MDA-MB-468 LGR4 KO cells. (B) WB analysis in MDA-MB-468 LGR4 KO cells. (C, D) Representative images (C) and quantification of transwell assay (D) showing that LGR4 knockout (KO) reduces MDA-MB-468 migration. Scale bar = 50 μm.

of 395 proteins were enriched in the WT group, and 362 proteins were enriched at 10 minutes. At 30 minutes, 368 proteins were enriched, including 258 intersecting proteins. A total of 365 proteins were pulled down in the KO group, with 314 proteins were enriched at 10 minutes, and 294 proteins enriched at 30 minutes, including 218 intersecting proteins.

Omics analysis revealed dynamic changes in EGFR-associated proteins in LGR4 WT/KO cells

In the WT proteome, 292 interacting proteins were divided into 4 clusters based on their binding kinetics (**Figure 4A**; Table S4). Enrichment analysis of each proteins cluster was performed (**Figure 4B**). Following EGF stimulation, Cluster 3 proteins such as ACTN1, CALD1, CAPZA1, GSN, MYH9 were continuously upregulated within 30 minutes, participating in the regulation of actin cytoskeleton, Rho GTPase pathway, and other actin-related pathways. Cluster 4 proteins, including ANK3, DSG2, NF2, TJP1, and ITGB4, showed increased abundance starting 10 minutes post-EGF stimulation, involved in cell junction and myomelament regulation. The LGR4 KO proteome contained 153 interacting proteins and 4 clusters associated with binding kinetics (**Figure 4C**; Table S5). Cluster 2 proteins such as CBL, GRB2, MAPK1, VAV2, and STAM were upregulated after EGF stimulation, peaking at 10 minutes before declining to a plateau, mainly regulating the EGFR signaling pathway. Cluster 3 proteins, including PIK3R1, PRKACK, PTPN11, PLK1, and SPRY4, were continuously increased in abundance within 30 minutes of EGF stimulation, primarily regulating the PIK3 pathway (**Figure 4D**).

Omics analysis highlighted defects in EGFR-dependent actin cytoskeletal organization in LGR4 KO cells

Pathway enrichment analysis of proteins obtained post-EGF stimulation at various time points in the LGR4 knockout breast cancer cell line (**Figure 5A**) indicated involvement in protein translation and intracellular protein transport in both WT and the KO cell lines, unaffected by LGR4 knockout. However, the actin cytoskeletal pathway showed a progressively sig-

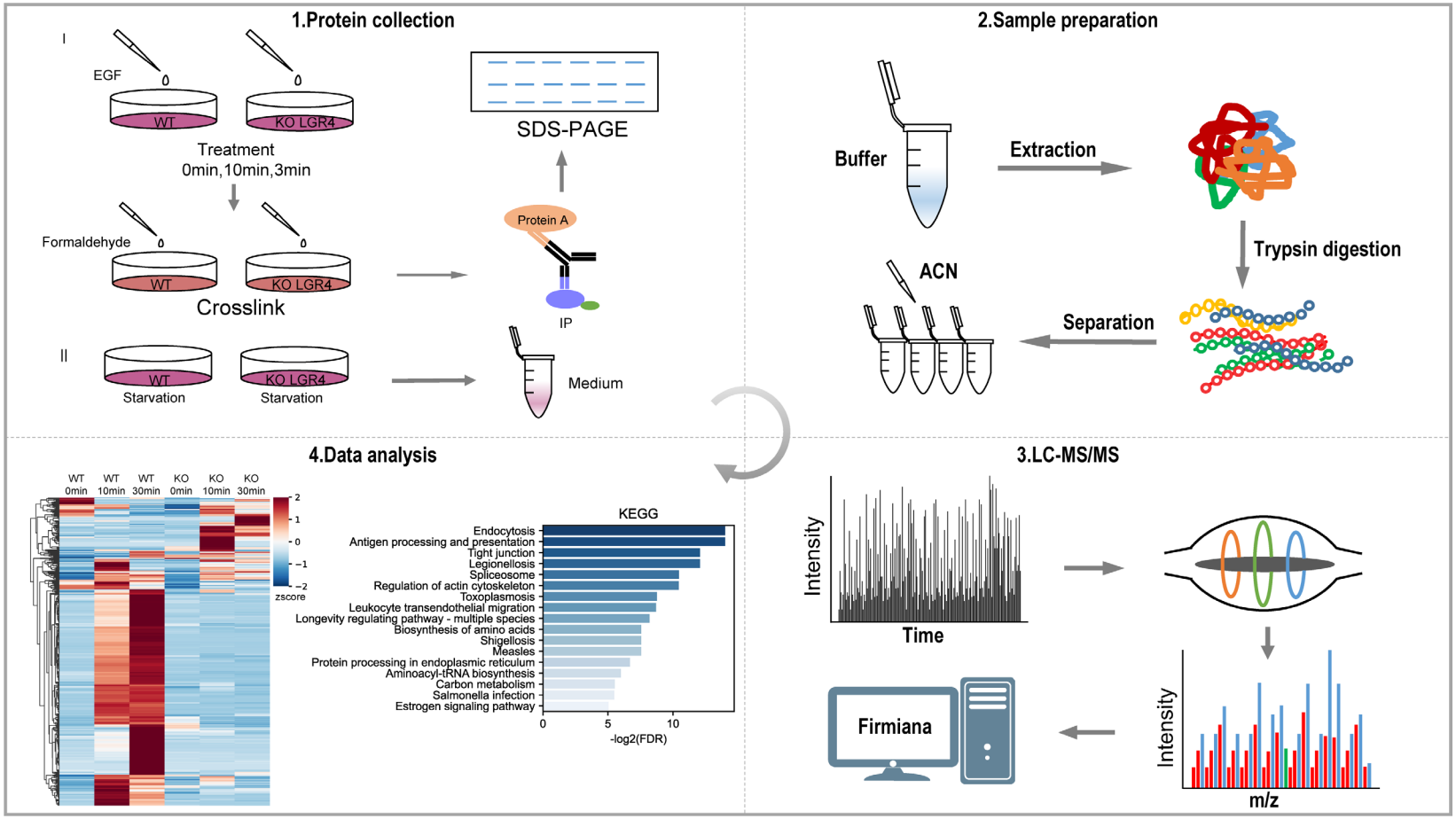

Figure 2. Schematics representation of the workflow for MS analysis of LGR4-dependent dynamic EGFR complexes and secretomes.

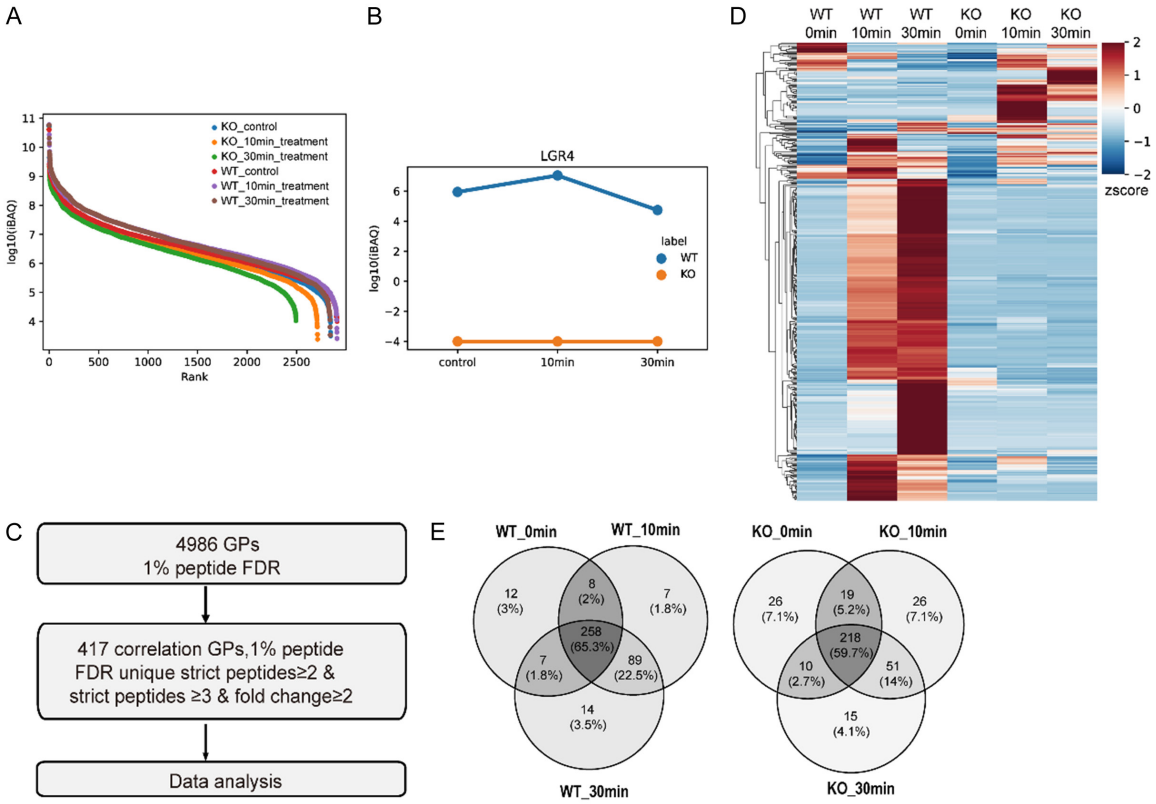

Figure 3. Proteomic landscape of dynamic EGFR-complexes in MDA-MB-468 cell lines. A. Dynamic ranges of proteomes measured at 3 time points. B. Abundance of LGR4 antigens in the MDA-MB-468 cell line. C. Multiple datasets using various filtering criteria. D. Heatmap of temporal proteomic data analyzed by unsupervised clustering and hierarchical clustering based on correlation. E. Venn diagram illustrating the overlap of proteins across 3 time points in both WT and KO groups.

nificant *p* value in the WT compared to the KO cell lines, indicating that there was a defect in EGFR-dependent actin cytoskeletal tissue in LGR4 knockout cell lines.

Protein abundance (**Figure 5B**) revealed that CBL protein peaked at 10 minutes post-stimulation in both WT and LGR4 knockout cells. Compared with the control group, GRB2 protein in the LGR4 knockout group peaked slightly faster than that of the control group, with both reaching the highest at 10 minutes. VSP11 protein, involved in protein transport regulation, showed the highest abundance at 10 minutes in both KO and WT lines. In contrast, ACTN1 protein, which is involved in the regulation of actin cytoskeletal tissue, was significantly reduced in knockout cells compared to WT lines. These studies suggest that LGR4 can regulate cytoskeletal proteins, thereby promoting EGF-EGFR activation-mediated tumor motility and migration, with higher expression correlating with likelihood of lymph nodes metastasize.

In addition, the enrichment analysis of up-regulated proteins after EGFR activation indicated that several biological processes, such as actin cytoskeleton and signal transduction of Rho GTPase pathway, were associated with secretory process [26, 27]. ARFIP2 protein, involved in vesicle-mediated transport and cytoskeletal remodeling, reached the highest at 10 minutes in WT cell lines, with levels remaining elevated at 30 minutes, in contrast to the KO cell line. Similarly, the protein abundance of EEA1 protein, which plays a crucial role in endocytosis and vesicle fusion, was significantly lower in KO cells than that of WT cell line at 10 minutes. The OPHN1 protein, which promotes GTP hydrolysis of Rho subfamily members, showed an increase in WT cell lines with extended EGF stimulation time. HIP1 protein, which plays a role in clathrin-mediated endocytosis and traf-

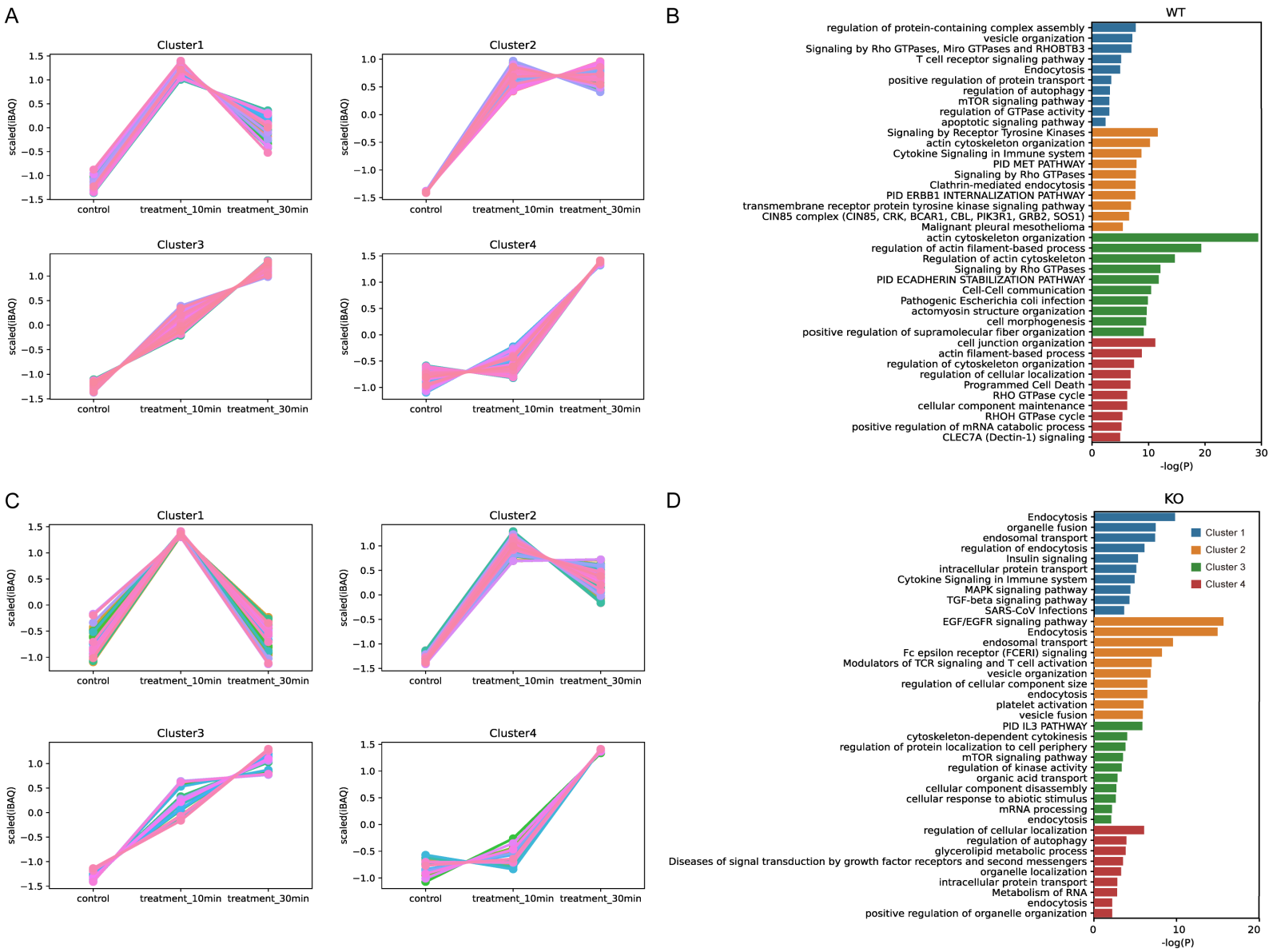

Figure 4. EGFR-association dynamics after EGF treatment in MDA-MB-468 WT and KO cells. (A) Protein trajectories for the 4 clusters in LGR4 WT cells. (B) Metascape term enrichments for the proteins in each cluster from (A). (C) Protein trajectories for the 4 clusters in LGR4 KO cells. (D) The Metascape term enrichments for the proteins in each cluster from (C).

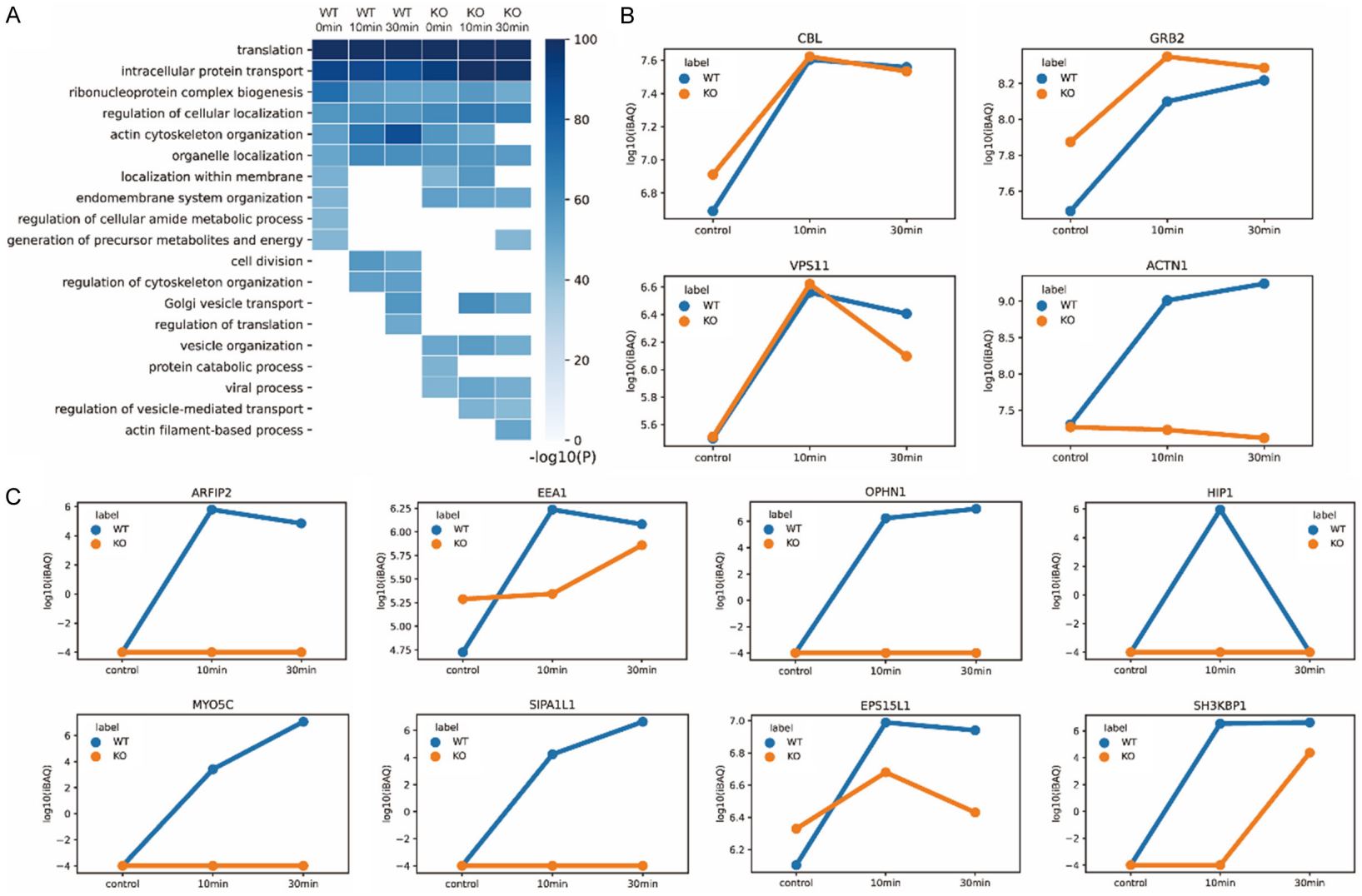

Figure 5. EGF-stimulated WT/KO cell lines at various time points. A. Protein pathway enrichment analysis. B. Line plots of protein abundance indicating representative core components over time. C. Abundance line plots of representative protein.

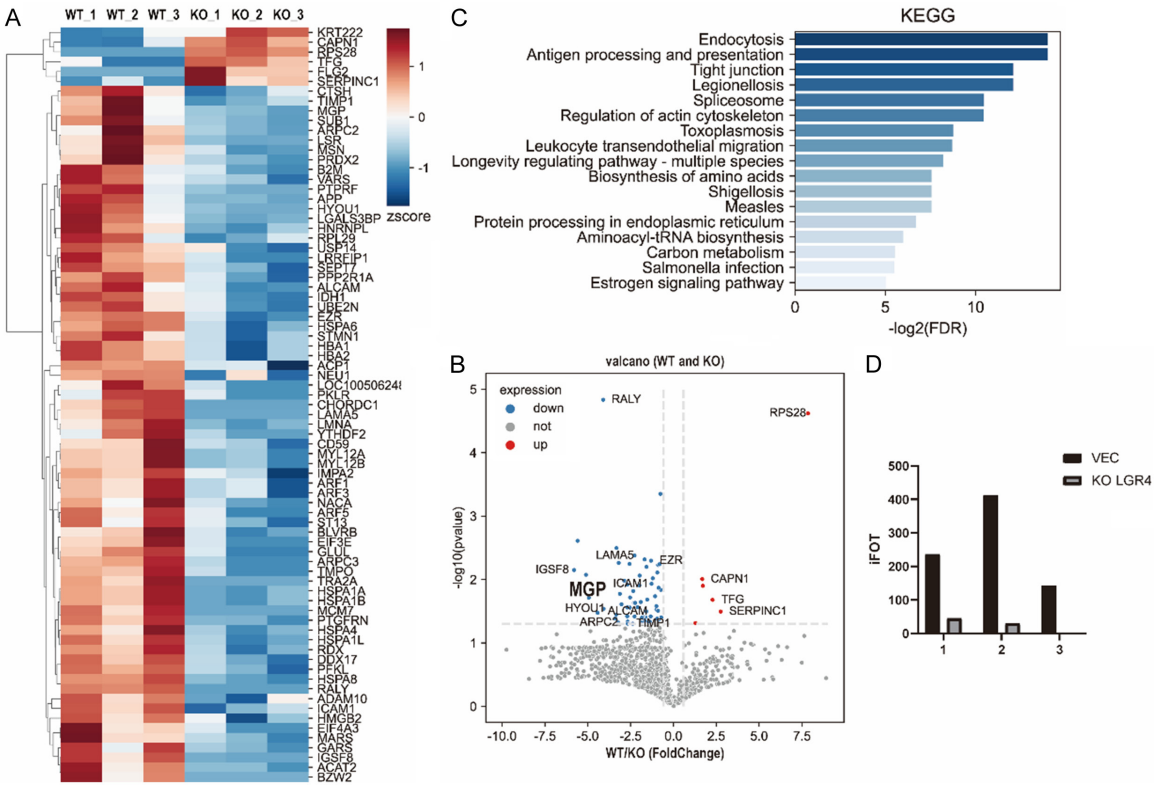

Figure 6. Secretory proteomic landscape of MDA-MB-468 cell lines. A. Heatmap of differential protein expression. B. Volcano plot of differential proteins. C. Enrichment analysis of down-regulated proteins. D. Histogram illustrating the fold down-regulation of MGP across three groups.

ficking, reached its peak at 10 minutes (**Figure 5C**). These observations suggest that the secretory process may be enhanced after EGF stimulation. Consequently, we began to study LGR4-dependent secretion proteomics and characterize the biologically significant proteins associated with this process.

Secreted protein profiling revealed that MGP might mediate the regulatory effect of LGR4 on migration

The conditioned media from the TNBC cell line MDA-MB-468 and its LGR4 knockout counterpart underwent mass spectrometry profiling (**Figure 2**). The raw data from 6 experimental samples were uploaded to the database for search, identifying a total of 2528 proteins (Table S6) in the secreted protein expression profile of LGR4 knockout. After strict quality control (p-value ≤ 0.05, fold change ≥ 1.5), 77 differential proteins were identified (**Figure 6A**), and volcanoes plotted were generated (**Figure 6B**). KEGG enrichment analysis of 71 down-regulated proteins (**Figure 6C**) revealed associations with processes such as tight junctions, endocytosis, actin regulation, and leukocyte transendothelial migration. Analysis of the differential proteins down-regulated in the LGR4 knockout data involved extensive literature review to elucidate the functions and current research status of each protein. Notably, matrix gla protein (MGP) was identified as high fold expression, as shown in **Figure 6D**, and is known to promote breast cancer migration [24]. At the secretory proteomic level, MGP appears to be a downstream effector mediating LGR4's ability to regulate migration. Subsequent investigations have begun to verify whether MGP is a downstream protein that mediates LGR4's ability to regulate migration at the cellular level began.

LGR4 knockdown reduces MGP protein expression

A stable MGP knockdown cell line was constructed in MDA-MB-468 cells. Both qPCR and Western blot analyses were performed (**Figure 7A**). Transwell experiments assays and subse-

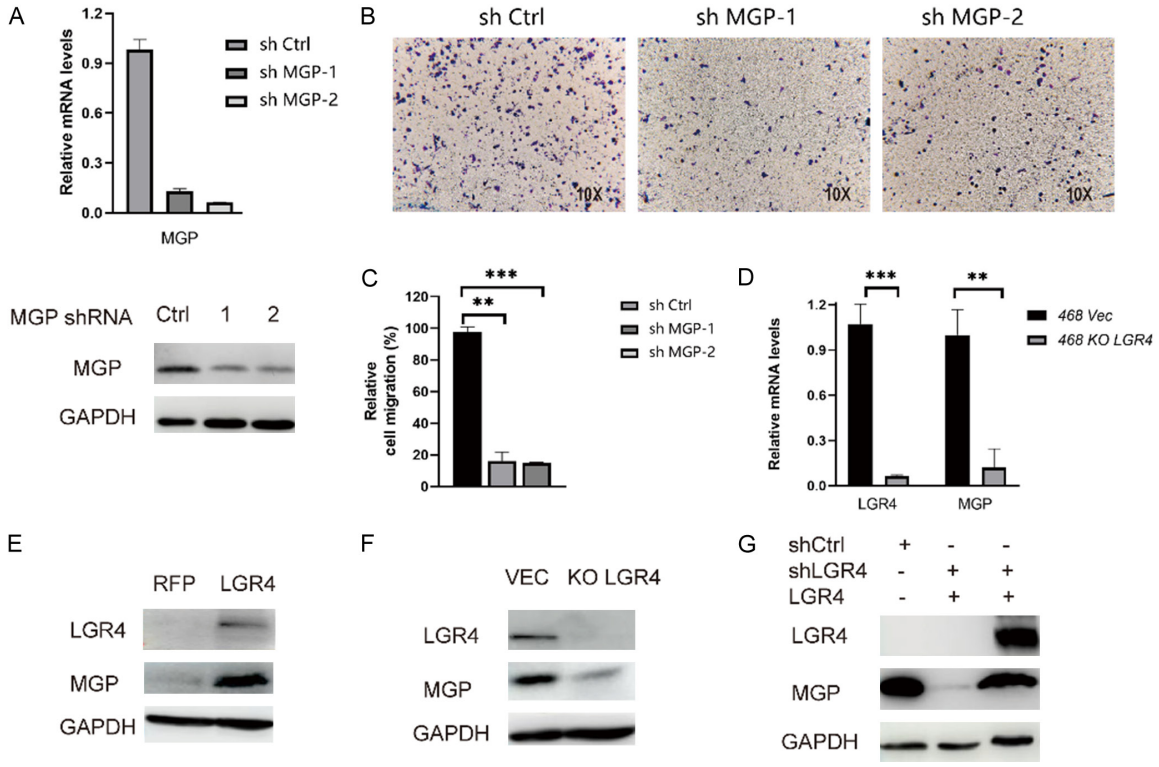

Figure 7. LGR4 knockdown reduces MGP protein expression. (A) qPCR and WB analysis in MDA-MB-468 MGP knockdown cells. (B, C) Representative images (B) and quantification (C) of transwell assay showing that MGP knockdown inhibits MDA-MB-468 migration. Scale bar = 100 μm. (D) qPCR analysis of MGP expression following LGR4 knockout. (E) WB analysis of MGP expression after LGR4 overexpression. (F) WB analysis of MGP expression levels post LGR4 knockout. (G) Changes in MGP protein following LGR4 knockout and subsequent LGR4 supplementation.

quent statistical analysis was performed for two groups of stable cells (**Figure 7B**). Compared to the control group, migration was significantly reduced in MGP knockdown cells, as evidenced by a significant *p*-value in the histogram (**Figure 7C**). Investigation of relationship between LGR4 and MGP at the cellular level revealed that LGR4 positively regulated MGP at the transcriptional level (**Figure 7D**). Decreases in LGR4 expression corresponded with reductions in MGP level, this relationship was consistent at both the transcriptional and protein levels (**Figure 7E** and **7F**). Furthermore, when LGR4 was reintroduced in LGR4-knockdown cells, MGP expression levels, previously diminished, were significantly rescued (**Figure 7G**).

Discussion

The main findings of this study are as follows: Firstly, LGR4 regulates cytoskeletal proteins, promoting EGF-EGFR activation, which mediated tumor motility and migration, thereby increasing the likelihood of lymph metastasis. Secondly, inhibition of LGR4 reduces EGFR activation-induced metastasis in TNBC by suppressing MGP expression.

LGR4, a highly conserved protein in the G protein coupled receptor (GPCR) family [28], which plays a significant role in various tumor development processes, including proliferation, migration, and apoptosis in cancers such as prostate [29, 30], ovarian cancer [31], glioma [32], and papillary thyroid cancer [33]. Previous studies have demonstrated that LGR4 mediates both tumorigenesis and metastasis in breast cancer [15].

The pathway protein study of LGR4 knockout breast cancer cell line revealed that the abundance of CBL protein peaked at 10 minutes post LGR4 knockout. CBL is recognized as the classical E3 ubiquitin ligase of EGFR [34], which mediates the ubiquitination and lysosomal degradation of EGFR [35]. It has been observed that inhibition of c-Cbl-mediated EGFR ubiquitination activates EGFR signaling pathway, which

in turn can promote migration, invasion, and liver metastasis in gallbladder cancer cells [36]. Moreover, studies have shown that c-cbl-mediated ubiquitination inhibits EGFR degradation, thereby promoting liver cancer metastasis [37]. This is consistent with the current understanding that LGR4 can promote breast cancer metastasis independent of Wnt signaling [18]. Furthermore, it was revealed that LGR4 can promote tumor motility and migration ability by regulating cytoskeletal proteins through EGF-EGFR activation.

MGP is a 10 Kda, vitamin K-dependent secreted protein consisting of 103 amino acids [38]. Although it belongs to the same Gla protein family as POSTN, MGP has been relatively underexplored but is increasingly recognized as a key factor in the development and progression of cancer. Studies have found that MGP can promote the growth and proliferation of colon cancer cells by increasing the concentration of free calcium ions within cells and activating the NF-kB pathway [39]. Additionally, MGP inhibits osteoblast mineralization and bone formation by regulating the deposition of the bone matrix [40]. It can also influence osteogenesis by upregulating the Wnt/β-Catenin signaling pathway [41]. MGP-induced epithelial-mesenchymal transition (EMT) promotes the proliferation and migration of TNBC cells. High MGP expression associates with poorer recurrence-free survival in TNBC patients [24].

Current studies have shown that MGP promotes the metastasis of breast cancer and regulate the formation of osteoclasts by regulating intracellular calcium ion flow. Concurrently, LGR4 has been shown to promote bone metastasis of breast cancer [16]. This suggests that MGP could be a downstream effector that mediates the LGR4's influence on migration. QPCR results showed that MGP protein expression increased following LGR4 overexpression and decreased with LGR4 downregulation. WB results analysis indicated that the MGP protein expression increased after LGR4 overexpression and decreased with LGR4 downregulation. Furthermore, when LGR4 was reintroduced into MDA-MD-468 with LGR4 knockdown, the previously diminished MGP protein levels were partially restored.

This study demonstrated that inhibition of LGR4 suppresses EGFR activation-induced TNBC metastasis by downregulating MGP expression. It also reveals the signaling regulation mechanism of LGR4 in TNBC cells, shedding light on the molecular mechanism through which LGR4 promotes metastasis. Additionally, the findings provides new targets for development of targeted therapies in cancer treatment.

Acknowledgements

This work was supported by the National Natural Science Foundation of China (No. 31970725).

Disclosure of conflict of interest

None.

Address correspondence to: Pumin Zhang, State Key Laboratory of Targeting Oncology, National Center for International Research of Biotargeting Theranostics, Guangxi Key Laboratory of Biotargeting Theranostics, Collaborative Innovation Center for Targeting Tumor Diagnosis and Therapy, Guangxi Medical University, Nanning 530021, Guangxi, PR China. E-mail: pzhangbcmedu@gmail.com; Yi Wang, State Key Laboratory of Proteomics, Beijing Proteome Research Center, National Center for Protein Sciences (Beijing), Beijing Institute of Lifeomics, Beijing 102206, PR China. E-mail: wangyi@ncpsb.org.cn

References

[1] Cancer Genome Atlas Network. Comprehensive molecular portraits of human breast tumours. Nature 2012; 490: 61-70.

[2] Allemani C, Matsuda T, Di Carlo V, Harewood R, Matz M, Nikšić M, Bonaventure A, Valkov M, Johnson CJ, Estève J, Ogunbiyi OJ, Azevedo e Silva G, Chen WQ, Eser S, Engholm G, Stiller CA, Monnereau A, Woods RR, Visser O, Lim GH, Aitken J, Weir HK and Coleman MP; CONCORD Working Group. Global surveillance of trends in cancer survival 2000-14 (CONCORD-3): analysis of individual records for 37 513 025 patients diagnosed with one of 18 cancers from 322 population-based registries in 71 countries. Lancet 2018; 391: 1023-1075.

[3] Valastyan S and Weinberg RA. Tumor metastasis: molecular insights and evolving paradigms. Cell 2011; 147: 275-292.

[4] Tulotta C and Ottewell P. The role of IL-1B in breast cancer bone metastasis. Endocr Relat Cancer 2018; 25: R421-R434.

[5] Xiong Z, Deng G, Huang X, Li X, Xie X, Wang J, Shuang Z and Wang X. Bone metastasis pattern in initial metastatic breast cancer: a population-based study. Cancer Manag Res 2018; 10: 287-295.
[6] Zhang W, Yu W, Cai G, Zhu J, Zhang C, Li S, Guo J, Yin G, Chen C and Kong L. Retracted Article: A new synthetic derivative of cryptotanshinone KYZ3 as STAT3 inhibitor for triple-negative breast cancer therapy. Cell Death Dis 2018; 9: 1098.
[7] Ghouse SM, Nguyen HM, Bommareddy PK, Guz-Montgomery K and Saha D. Oncolytic herpes simplex virus encoding IL12 controls triple-negative breast cancer growth and metastasis. Front Oncol 2020; 10: 384.
[8] Luo Y, Zhang W, Xu L, Chen Y, Xu Y and Yuan L. Long non-coding RNA PVT1 regulates the resistance of the breast cancer cell line MDA-MB-231 to doxorubicin via Nrf2. Technol Cancer Res Treat 2020; 19: 1533033820980763.
[9] Goidts V, Nakata S and Phillips E. Emerging role for leucine-rich repeat-containing G-protein-coupled receptors LGR5 and LGR4 in cancer stem cells. Cancer Manag Res 2014; 6: 171-180.
[10] Mohri Y, Umezu T, Hidema S, Tomisawa H, Akamatsu A, Kato S, Nawa A and Nishimori K. Reduced fertility with impairment of early-stage embryos observed in mice lacking Lgr4 in epithelial tissues. Fertil Steril 2010; 94: 2878-2881.
[11] Kinzel B, Pikiolek M, Orsini V, Sprunger J, Isken A, Zietzling S, Desplanches M, Dubost V, Breustedt D, Valdez R, Liu D, Theil D, Müller M, Dietrich B, Bouwmeester T, Ruffner H and Tchorz JS. Functional roles of Lgr4 and Lgr5 in embryonic gut, kidney and skin development in mice. Dev Biol 2014; 390: 181-190.
[12] Mohri Y, Kato S, Umezawa A, Okuyama R and Nishimori K. Impaired hair placode formation with reduced expression of hair follicle-related genes in mice lacking Lgr4. Dev Dyn 2008; 237: 2235-2242.
[13] Luo J, Yang Z, Ma Y, Yue Z, Lin H, Qu G, Huang J, Dai W, Li C, Zheng C, Xu L, Chen H, Wang J, Li D, Siwko S, Penninger JM, Ning G, Xiao J and Liu M. LGR4 is a receptor for RANKL and negatively regulates osteoclast differentiation and bone resorption. Nat Med 2016; 22: 539-546.
[14] Ordaz-Ramos A, Rosales-Gallegos VH, Melendez-Zajgla J, Maldonado V and Vazquez-Santillan K. The role of LGR4 (GPR48) in normal and cancer processes. Int J Mol Sci 2021; 22: 4690.
[15] Yue Z, Yuan Z, Zeng L, Wang Y, Lai L, Li J, Sun P, Xue X, Qi J, Yang Z, Zheng Y, Fang Y, Li D, Siwko S, Li Y, Luo J and Liu M. LGR4 modulates breast cancer initiation, metastasis, and cancer stem cells. FASEB J 2018; 32: 2422-2437.
[16] Yue Z, Niu X, Yuan Z, Qin Q, Jiang W, He L, Gao J, Ding Y, Liu Y, Xu Z, Li Z, Yang Z, Li R, Xue X, Gao Y, Yue F, Zhang XH, Hu G, Wang Y, Li Y, Chen G, Siwko S, Gartland A, Wang N, Xiao J, Liu M and Luo J. RSPO2 and RANKL signal through LGR4 to regulate osteoclastic premetastatic niche formation and bone metastasis. J Clin Invest 2022; 132: e144579.
[17] Liu S, Gao Y, Zhang L, Yin Y and Zhang W. Rspo1/Rspo3-LGR4 signaling inhibits hepatic cholesterol synthesis through the AMPKα-SREBP2 pathway. FASEB J 2020; 34: 14946-14959.
[18] Yue F, Jiang W, Ku AT, Young AIJ, Zhang W, Souto EP, Gao Y, Yu Z, Wang Y, Creighton CJ, Nagi C, Wang T, Hilsenbeck SG, Feng XH, Huang S, Coarfa C, Zhang XH, Liu Q, Lin X and Li Y. A Wnt-independent LGR4-EGFR signaling axis in cancer metastasis. Cancer Res 2021; 81: 4441-4454.
[19] Burness ML, Grushko TA and Olopade OI. Epidermal growth factor receptor in triple-negative and basal-like breast cancer: promising clinical target or only a marker? Cancer J 2010; 16: 23-32.
[20] Sigismund S, Avanzato D and Lanzetti L. Emerging functions of the EGFR in cancer. Mol Oncol 2018; 12: 3-20.
[21] González-González L and Alonso J. Periostin: a matricellular protein with multiple functions in cancer development and progression. Front Oncol 2018; 8: 225.
[22] Nishimoto SK and Nishimoto M. Matrix gla protein binds to fibronectin and enhances cell attachment and spreading on fibronectin. Int J Cell Biol 2014; 2014: 807013.
[23] Kudo A. Periostin in fibrillogenesis for tissue regeneration: periostin actions inside and outside the cell. Cell Mol Life Sci 2011; 68: 3201-3207.
[24] Gong C, Zou J, Zhang M, Zhang J, Xu S, Zhu S, Yang M, Li D, Wang Y, Shi J and Li Y. Upregulation of MGP by HOXC8 promotes the proliferation, migration, and EMT processes of triple-negative breast cancer. Mol Carcinog 2019; 58: 1863-1875.
[25] Chen Y, Leng M, Gao Y, Zhan D, Choi JM, Song L, Li K, Xia X, Zhang C, Liu M, Ji S, Jain A, Saltzman AB, Malovannaya A, Qin J, Jung SY and Wang Y. A cross-linking-aided immunoprecipitation/mass spectrometry workflow reveals extensive intracellular trafficking in time-resolved, signal-dependent epidermal growth factor receptor proteome. J Proteome Res 2019; 18: 3715-3730.
[26] Calvo V and Izquierdo M. Role of actin cytoskeleton reorganization in polarized secretory traf-

fic at the immunological synapse. Front Cell Dev Biol 2021; 9: 629097.
[27] Streit L, Brunaud L, Vitale N, Ory S and Gasman S. Hormones secretion and Rho GTPases in neuroendocrine tumors. Cancers (Basel) 2020; 12: 1859.
[28] Dorsam RT and Gutkind JS. G-protein-coupled receptors and cancer. Nat Rev Cancer 2007; 7: 79-94.
[29] Luo W, Tan P, Rodriguez M, He L, Tan K, Zeng L, Siwko S and Liu M. Leucine-rich repeat-containing G protein-coupled receptor 4 (Lgr4) is necessary for prostate cancer metastasis via epithelial-mesenchymal transition. J Biol Chem 2017; 292: 15525-15537.
[30] Liang F, Yue J, Wang J, Zhang L, Fan R, Zhang H and Zhang Q. GPCR48/LGR4 promotes tumorigenesis of prostate cancer via PI3K/Akt signaling pathway. Med Oncol 2015; 32: 49.
[31] Zeng Z, Ji N, Yi J, Lv J, Yuan J, Lin Z, Liu L and Feng X. LGR4 overexpression is associated with clinical parameters and poor prognosis of serous ovarian cancer. Cancer Biomark 2020; 28: 65-72.
[32] Yu CY, Liang GB, Du P and Liu YH. Lgr4 promotes glioma cell proliferation through activation of Wnt signaling. Asian Pac J Cancer Prev 2013; 14: 4907-4911.
[33] Kang YE, Kim JM, Kim KS, Chang JY, Jung M, Lee J, Yi S, Kim HW, Kim JT, Lee K, Choi MJ, Kang SK, Lee SE, Yi HS, Koo BS and Shong M. Upregulation of RSPO2-GPR48/LGR4 signaling in papillary thyroid carcinoma contributes to tumor progression. Oncotarget 2017; 8: 114980-114994.
[34] Zhao L, Qiu T, Jiang D, Xu H, Zou L, Yang Q, Chen C and Jiao B. SGCE promotes breast cancer stem cells by stabilizing EGFR. Adv Sci (Weinh) 2020; 7: 1903700.
[35] Zhao XC, Wang GZ, Wen ZS, Zhou YC, Hu Q, Zhang B, Qu LW, Gao SH, Liu J, Ma L, Zhang YF, Zhang C, Yu H, Zhang DL, Wang M, Wang CL, Huang YC, Liu ZH, Zhao Y, Chen L and Zhou GB. Systematic identification of CDC34 that functions to stabilize EGFR and promote lung carcinogenesis. EBioMedicine 2020; 53: 102689.
[36] Shen H, He M, Lin R, Zhan M, Xu S, Huang X, Xu C, Chen W, Yao Y, Mohan M and Wang J. PLEK2 promotes gallbladder cancer invasion and metastasis through EGFR/CCL2 pathway. J Exp Clin Cancer Res 2019; 38: 247.
[37] Zhang S, Jia X, Dai H, Zhu X, Song W, Bian S, Wu H, Chen S, Tang Y, Chen J, Jin C, Zhou M, Xie H, Zheng S and Song P. SERPINE2 promotes liver cancer metastasis by inhibiting c-Cbl-mediated EGFR ubiquitination and degradation. Cancer Commun (Lond) 2024; 44: 384-407.
[38] Balbino KP, Hermsdorff HHM and Bressan J. Polymorphism related to cardiovascular risk in hemodialysis subjects: a systematic review. J Bras Nefrol 2018; 40: 179-192.
[39] Li X, Wei R, Wang M, Ma L, Zhang Z, Chen L, Guo Q, Guo S, Zhu S, Zhang S and Min L. MGP promotes colon cancer proliferation by activating the NF-κB pathway through upregulation of the calcium signaling pathway. Mol Ther Oncolytics 2020; 17: 371-383.
[40] Zhang Y, Zhao L, Wang N, Li J, He F, Li X and Wu S. Unexpected role of matrix gla protein in osteoclasts: inhibiting osteoclast differentiation and bone resorption. Mol Cell Biol 2019; 39: e00012-00019.
[41] Zhang J, Ma Z, Yan K, Wang Y, Yang Y and Wu X. Matrix gla protein promotes the bone formation by up-regulating Wnt/β-catenin signaling pathway. Front Endocrinol (Lausanne) 2019; 10: 891.

Table S1. Primers used in the study

Oligonucleotides
Primers specific for LGR4 in real-time PCR
F: ACCTGGAGACCTTAGACTTG
R: CCACGAATGACTAGGGAATG
Primers specific for MGP in real-time PCR
F: AGAACGCTCTAAGCCTGTCCA
R: GGCAGCATTGTATCCATAAACC
Primers specific for GAPDH in real-time PCR
F: GAGGGCTGCTTTTAACTCTGG
R: GATTTTGGAGGGATCTCGCT
Primers specific for full-length LGR4
F: CCGGAATTCATGGATTACAAGGACGATGACAAGATGCCGGGCCCGCTAGGGCT
G: CGCGGATCCTCACTTGTCATCGTCGTCCTTGTAATCCATGTCTTTAACTCTTGGTAGAT
LGR4 sgRNA fragments inserted into LentiCRISPRv2 plasmid
sgLGR4-1: CTGCGACGGCGACCGTCGGG
sgLGR4-2: TACCCAGTGAAGCCATTCGA
sgLGR4-3: GGGCTGACGGCCGTGCCCGA
MGP shRNA fragments inserted into pLKO.1 plasmid
shMGP-1-F: CCGGCATGAAAGCATGGAATCTTATCTCGAGATAA GATTCCATGCTTTCATGTTTTTG
shMGP-1-R: AATTCAAAAACATGAAAGCATGGAATCTTATCTCG AGATAAGATTCCATGCTTTCATG
shMGP-2-F: CCGGA GCCTGTCCACGAGCTCAATACTCGAGTATTGAGCTCGTGGACAGGCTTTTTTG
shMGP-2-R: AATTCAAAAAAGCCTGTCCACGAGCTCAATACTCGAGTATTGAGCTCGTGGACAGGCT
LGR4 shRNA fragments inserted into pLKO.1 plasmid
shLGR4--F: CCGGCAAAGAACAGGTGCCTAAATTCTCGAGAATTTA GGCACCTGTTCTTTGTTTTTTG
shLGR4-R: AATTCAAAAAACAAAGAACAGGTGCCTAAATTCTCGAGAATTTAGGCACCTGTTCTTTG